

Microspectrophotometry of visual pigments and oil droplets in a marine bird, the wedge-tailed shearwater *Puffinus pacificus*: topographic variations in photoreceptor spectral characteristics

Nathan S. Hart*

Vision, Touch and Hearing Research Centre, School of Biomedical Sciences, University of Queensland, Brisbane, Queensland 4072, Australia

*e-mail: n.hart@uq.edu.au

Accepted 5 January 2004

Summary

Microspectrophotometric examination of the retina of a procellariiform marine bird, the wedge-tailed shearwater *Puffinus pacificus*, revealed the presence of five different types of vitamin A₁-based visual pigment in seven different types of photoreceptor. A single class of rod contained a medium-wavelength sensitive visual pigment with a wavelength of maximum absorbance (λ_{\max}) at 502 nm. Four different types of single cone contained visual pigments maximally sensitive in either the violet (VS, λ_{\max} 406 nm), short (SWS, λ_{\max} 450 nm), medium (MWS, λ_{\max} 503 nm) or long (LWS, λ_{\max} 566 nm) spectral ranges. In the peripheral retina, the SWS, MWS and LWS single cones contained pigmented oil droplets in their inner segments with cut-off wavelengths (λ_{cut}) at 445 (C-type), 506 (Y-type) and 562 nm (R-type), respectively. The VS visual pigment was paired with a transparent (T-type) oil droplet that displayed no significant absorption above at least 370 nm. Both the principal and accessory members of the double cone pair contained the same 566 nm λ_{\max} visual pigment as the LWS single cones but

only the principal member contained an oil droplet, which had a λ_{cut} at 413 nm. The retina had a horizontal band or 'visual streak' of increased photoreceptor density running across the retina approximately 1.5 mm dorsal to the top of the pecten. Cones in the centre of the horizontal streak were smaller and had oil droplets that were either transparent/colourless or much less pigmented than at the periphery. It is proposed that the reduction in cone oil droplet pigmentation in retinal areas associated with high visual acuity is an adaptation to compensate for the reduced photon capture ability of the narrower photoreceptors found there. Measurements of the spectral transmittance of the ocular media reveal that wavelengths down to at least 300 nm would be transmitted to the retina.

Key words: colour vision, MSP, microspectrophotometry, spectral sensitivity, petrel, shearwater, *Puffinus pacificus*, procellariiform, seabird, ocular media, visual ecology.

Introduction

The nature of colour vision varies throughout the animal kingdom, as does the morphological structure of the eye, and this great diversity in ocular design is thought to represent adaptations to different life styles (Walls, 1942; Rochon-Duvigneaud, 1943; Meyer, 1977; Lythgoe, 1979). Our understanding of colour vision in birds is derived from only a handful of species, but it is evident that there is considerable interspecific variation in retinal design (e.g. Slonaker, 1897; Wood, 1917; Goldsmith et al., 1984; Martin, 1985; Partridge, 1989; Bowmaker et al., 1997; Hart, 2001a,b; Ödeen and Håstad, 2003). Nevertheless, in order to establish which features of the avian retina are adaptive for specific visual tasks it is necessary to obtain data from more species.

Only 3% of the world's birds are classified as seabirds (Nelson, 1980), but their highly specialized life styles may provide some insights into avian retinal design. However, while the optical structure of the eyes of marine species has

received considerable attention (Sivak, 1976; Sivak et al., 1977, 1987; Martin and Brooke, 1991; Martin, 1998, 1999; Martin and Prince, 2001), only limited and partial data are available on their photoreceptor spectral sensitivities (Liebman, 1972; Bowmaker and Martin, 1985; Bowmaker et al., 1997; Ödeen and Håstad, 2003). Described here are new data on the spectral absorption characteristics of the visual pigments and cone oil droplets in the retinal photoreceptors of the wedge-tailed shearwater *Puffinus pacificus*, measured using microspectrophotometry. The wedge-tailed shearwater is a marine pelagic species that spends most of its life on the open ocean, approaching land only long enough to breed (Schodde and Tidemann, 1997). During the day, shearwaters forage low over the sea's surface looking for fish, crustaceans and cephalopods. Although predominantly diurnal in habit, they may come ashore after dark during the breeding season (Warham, 1990).

Materials and methods

Animals

Three fledgling wedge-tailed shearwaters *Puffinus pacificus* (Gmelin 1789) were caught under Queensland Parks and Wildlife Service Permit (WITK00494802) on Heron Island (Queensland, Australia) during May 2003. They had become entangled in *Pisonia grandis* seeds but were otherwise undamaged. Birds were held in darkness for at least 1 h prior to killing by approved humane methods (overdose of barbiturate anaesthetic followed immediately by decapitation). All procedures were conducted on Heron Island and were approved by the University of Queensland Animal Ethics Committee.

Microspectrophotometry of photoreceptors

Following enucleation, dark-adapted eyes were dissected in 340 mOsmol kg⁻¹ phosphate-buffered saline (PBS; Oxoid, Basingstoke, UK) and retinal tissue prepared for analysis with a microspectrophotometer as described elsewhere (Hart et al., 1998, 1999, 2000a,b; Hart, 2002). Photoreceptors were mounted in a solution of 340 mOsmol kg⁻¹ PBS containing 10% dextran (MW 282,000; Sigma D-7265). All preparations were conducted under infrared (IR) illumination provided by a bank of IR light-emitting diodes (LEDs) and visualized using an IR image converter (FJW Optical Systems Inc., Palatine, IL, USA).

The microspectrophotometer (MSP) used was a new field-portable single-beam wavelength-scanning instrument of simple design constructed by the author. The filament of a 12 V 50 watt tungsten halogen lamp was focused by a biconvex quartz lens (focal length $f=50$ mm) onto the entrance slit (1 mm width) of a Jobin-Yvon H10-61 UV-VIS monochromator (JY Horiba, France). The monochromator contained a directly driven, concave, holographic grating that dispersed the incident light and focused the diffracted wavefront onto the exit slit (1 mm width). An image of the exit slit was projected by another $f=50$ mm biconvex quartz lens onto a variable rectangular field aperture that controlled the dimensions of the measuring beam (minimum 1 $\mu\text{m}\times 1$ μm). Light passing through the aperture was linearly polarized to take advantage of the inherent dichroism of photoreceptor outer segments when illuminated side-on. An image of the aperture was demagnified and focused into the plane of a specimen on a micrometer-manipulated microscope stage using a Zeiss (Germany) $\times 40$ 0.75 numerical aperture (NA) water immersion objective. Above the stage, a Leitz (Germany) $\times 100$ 1.32 NA oil immersion objective imaged the measuring beam onto the photocathode of a photomultiplier tube (PMT; Model R928, Hamamatsu, Japan) or, *via* a sliding mirror that could be introduced to the beam path, onto the image plane of a black and white charge-coupled device (CCD) video camera. To view the specimen using the CCD camera, light (>900 nm) from an IR LED was directed into the beam path using a fixed 45° beamsplitter (19 mm diameter No. 0 coverglass; ProSciTech, Australia) positioned below the condenser objective.

To compensate for longitudinal chromatic aberration in the

condenser objective, which would otherwise cause defocus of the measuring beam in the specimen plane when scanning through the spectrum (between 370 nm and 800 nm), a MIPOS 3 SG piezoelectric translator and 12 V 40 SG piezo amplifier (Piezosystem, Jena, Germany) were used to move the condenser automatically during the scan. The wavelength calibration of the MSP was checked with a calibrated Ocean Optics USB2000 spectroradiometer (Ocean Optics Inc., Dunedin, FL, USA) and was accurate to better than ± 1 nm.

Sample and baseline scans were made from cellular and tissue-free regions of the preparation, respectively. Dimensions of the measuring beam varied from approximately 1 $\mu\text{m}\times 1$ μm for oil droplets and small cone outer segments to 2 $\mu\text{m}\times 10$ μm for rods. The photocurrent induced by light from the measuring beam reaching the photomultiplier was converted to a voltage by a transimpedance headstage amplifier (Hamamatsu C6271, Schizuoka, Japan) and differentially amplified to reject common-mode voltages. The voltage was further amplified and scaled to suit the input range of a 12-bit successive-approximation sample and hold analogue-to-digital converter that was subsequently interrogated by a Gateway laptop microcomputer *via* the parallel port. Each scan consisted of a 'downward' long- to short-wavelength pass and an 'upward' short- to long-wavelength spectral pass. Corresponding wavelength data from the downward and upward spectral passes were averaged together. To reduce the effects of in-scan bleaching, only one sample scan was made of a given outer segment and this was combined with a single baseline scan. Following these 'pre-bleach' scans, outer segments were bleached with full spectrum 'white' light from the monochromator for 3 min and an identical number of sample and baseline scans made subsequently. The 'post-bleach' spectrum thus created was deducted from the pre-bleach spectrum to create a bleaching difference spectrum for each outer segment. To establish visual pigment-oil droplet pairings, the spectral absorbance of the oil droplet associated with the outer segment (if present) was also measured in the same way.

Analysis of visual pigment absorbance spectra

Baseline and sample data were converted to absorbance values at each wavelength and spectra normalized to the peak and long-wavelength offset absorbances determined by fitting a variable-point unweighted running average to the data (Hart, 1998). A regression line was fitted to the normalized absorbance data between 30% and 70% of the normalized maximum on the long-wavelength limb and the regression equation used to predict the wavelength of maximum absorbance (λ_{max}) following the methods of MacNichol (1986) and Govardovskii et al. (2000). Spectra from each photoreceptor type that satisfied established selection criteria (Levine and MacNichol, 1985; Hart et al., 1999) were averaged and reanalysed. For display, averaged spectra were overlaid with a rhodopsin (vitamin A₁-based) visual pigment template of the same λ_{max} generated using the equations of Govardovskii et al. (2000).

Analysis of oil droplet absorbance spectra

Sample and baseline data were converted to absorbance and normalized to the maximum and long-wavelength offset absorbances obtained by fitting an 11-point unweighted running average to the data. Oil droplet absorbance spectra were described by their cut-off wavelength (λ_{cut}), which is the

wavelength of the intercept at the value of maximum measured absorbance by the line tangent to the oil droplet absorbance curve at half maximum measured absorbance (Lipetz, 1984a). For comparison with other studies (e.g. Partridge, 1989) the wavelength corresponding to half maximum measured absorbance (λ_{mid}) was also calculated (Lipetz, 1984a).

Measuring spectral transmittance of the ocular media

The spectral transmittance (250–800 nm) of the ocular media in the anterior segment of the eye (cornea, aqueous humour and lens) was measured along the optical axis using an Ocean Optics S2000 spectroradiometer. Broad spectrum white light from an Ocean Optics PX-2 pulsed xenon lamp was delivered to either the corneal or lenticular aspects of the anterior segment of a hemisected eye at normal incidence using a 1 mm diameter fibre optic. The anterior segment was supported on a hollow metal tube (10 mm in length and 5 mm internal diameter) screwed onto the sub-miniature type A (SMA) connector of a 0.4 mm diameter fibre optic that relayed transmitted light to the S2000. Data collection was controlled via a Toshiba laptop microcomputer. After correcting the S2000 for electrical dark current, sample and baseline readings were made – with and without the anterior segment of the eye in the beam path, respectively – and converted to transmittance. In total, 13 spectra were obtained from the anterior segment of a single eye; of these, six were illuminated from the corneal aspect and seven from the lenticular aspect. All spectra were interpolated at 1 nm wavelength intervals, smoothed using an 11-point unweighted running average and averaged together.

Results*Appearance of the retina*

Macroscopic examination of the fundus of the shearwater eye revealed an obvious visual streak approximately 1.5 mm dorsal to the top of the pecten that ran horizontally across the retina. Microscopic examination of the dissected retina showed that the photoreceptors in the visual streak (Fig. 1C) were smaller and more densely packed than in the peripheral retina (Fig. 1A). Moreover, the pigmentation of the oil droplets found in the cone photoreceptors in the visual streak was greatly reduced compared to those found in the peripheral retina. There were, for instance, no bright yellow or red oil droplets in the centre of the visual streak. The transition from heavily pigmented to pale-coloured oil droplets occurred on the edge of the visual streak (Fig. 1B).

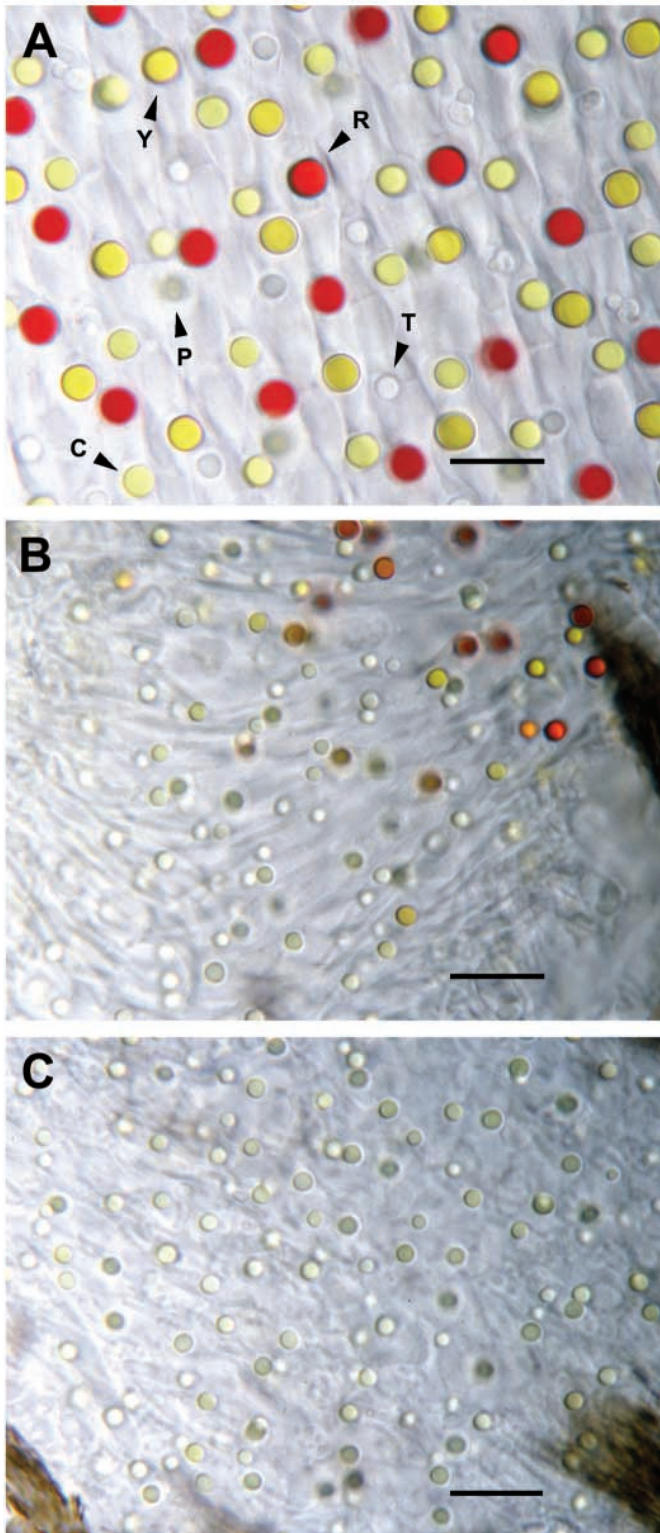


Fig. 1. Photomicrographs of the wedge-tailed shearwater *Puffinus pacificus* retina showing the appearance of the cone oil droplets in the periphery (A), on the edge of the visual streak (B) and in the centre of the visual streak (C). T, C, Y, R and P refer to the oil droplets found in the VS, SWS, MWS and LWS single cones and the principal member of the double cones, respectively. The P type droplets are out of focus as they are situated at a more sclerad level than the single cone oil droplets. All images were taken at the same magnification; scale bars, 10 μm .

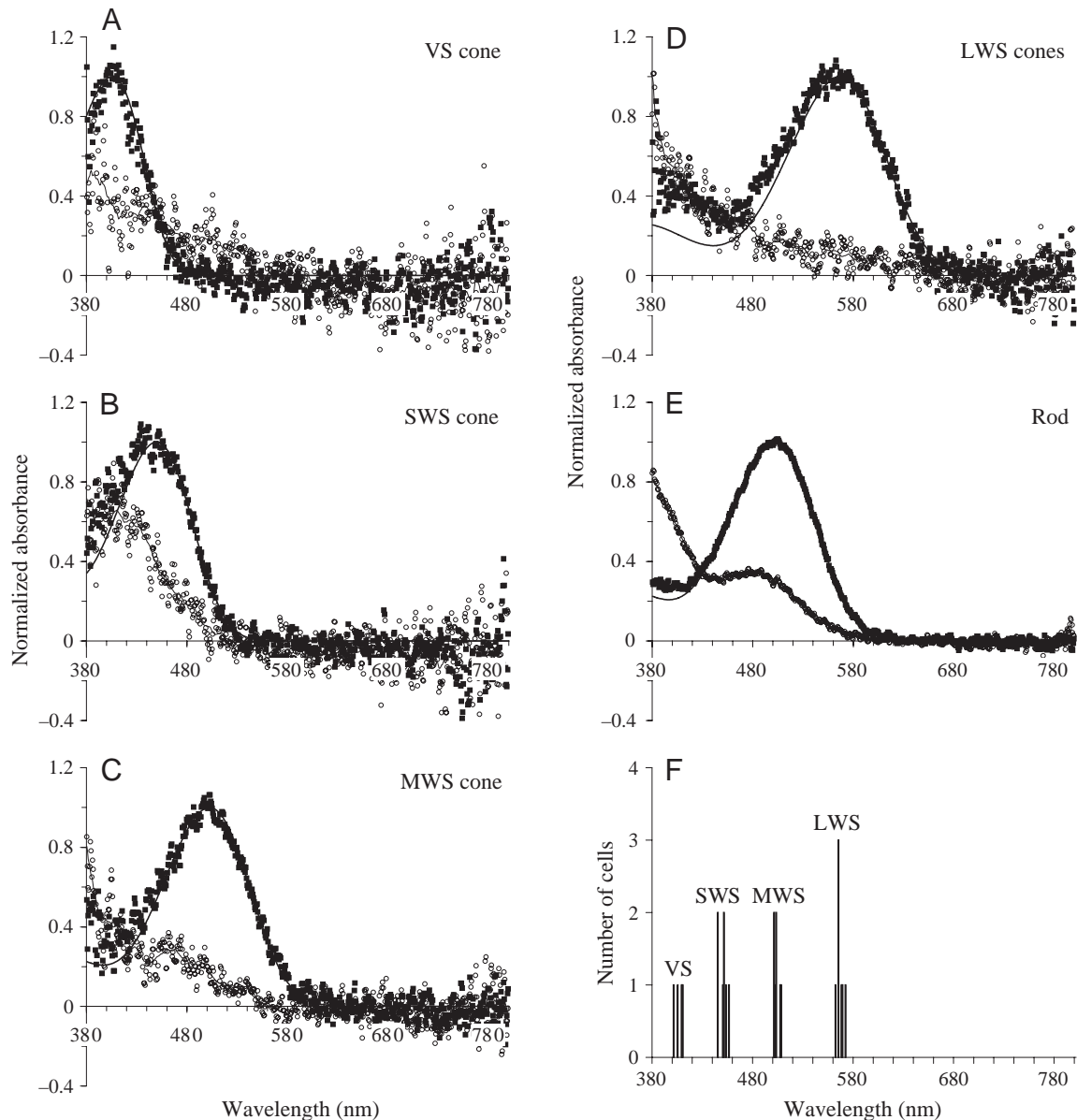


Fig. 2. (A–E) Normalized mean pre-bleach (filled squares) and post-bleach (open circles) absorbance spectra of the photoreceptor visual pigments in the wedge-tailed shearwater *Puffinus pacificus*. Pre-bleach spectra are overlaid with best-fitted rhodopsin templates (bold lines; Govardovskii et al., 2000). Post-bleach absorbance spectra are fitted with a variable-point running average (thin lines). The mean LWS spectrum (D) includes data from the LWS single cones and both the principal and accessory members of the LWS double cone pair. (F) Histogram showing the spectral distribution of the wavelengths of maximum absorbance (λ_{\max}) of the individual cone visual pigment spectra used to create the mean spectra. VS, SWS, MWS and LWS refer to violet-, short-, medium- and long-wavelength sensitive visual pigments, respectively.

Microspectrophotometry

Microspectrophotometric data for visual pigments (Figs 2, 3) and oil droplets (Fig. 4) measured outside the visual streak are summarized in Table 1. The retina of the wedge-tailed shearwater contained five different types of visual pigment in seven different classes of photoreceptor. On the basis of goodness-of-fit to visual pigment templates (Govardovskii et al., 2000), all of the visual pigments were considered to be rhodopsins, where the chromophore is 11-*cis* retinal. Rods contained a medium-wavelength sensitive (MWS) visual

pigment with a λ_{\max} at 502 nm. There were four spectrally distinct types of single cone. Firstly, a violet sensitive (VS) type with a 406 nm λ_{\max} visual pigment and a ‘transparent’ T-type oil droplet that showed no significant absorbance down to at least 370 nm. Secondly, a short-wavelength sensitive (SWS) type with a 450 nm λ_{\max} visual pigment and a pale greenish-yellow C-type oil droplet with a λ_{cut} at 445 nm. Thirdly, a MWS type with a 503 nm λ_{\max} visual pigment and a golden yellow Y-type oil droplet with a λ_{cut} at 506 nm. Lastly, a long-wavelength sensitive (LWS) type with a 566 nm

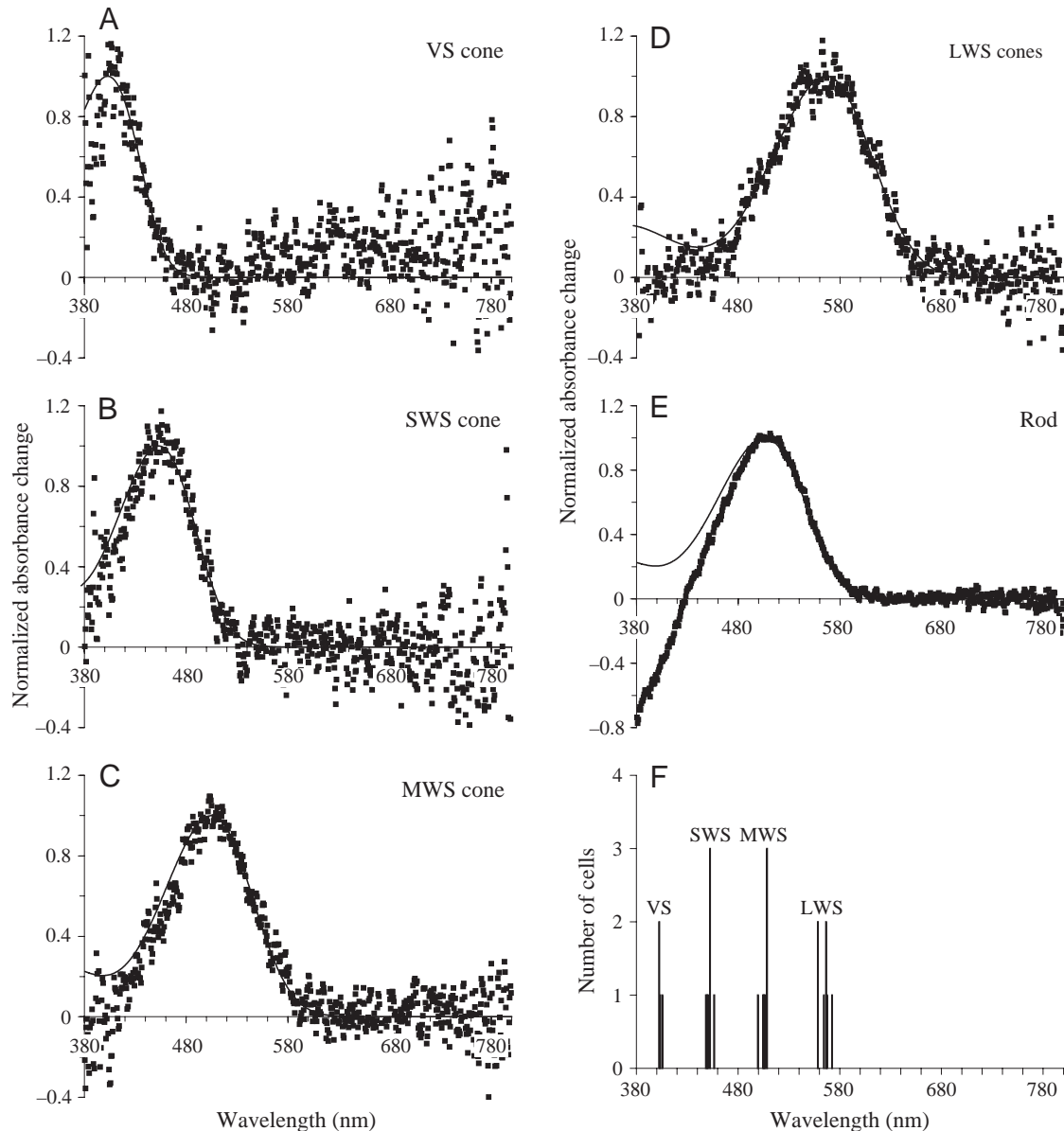


Fig. 3. (A–E) Normalized mean difference spectra (symbols) and best-fitted rhodopsin visual pigment templates (lines) for the photoreceptor visual pigments in the wedge-tailed shearwater *Puffinus pacificus*. Difference spectra represent the change in absorbance of the outer segment on bleaching with white light (see text for details). (F) Histogram showing the spectral distribution of the wavelengths of maximum absorbance (λ_{max}) of the individual cone visual pigment difference spectra used to create the mean spectra. For further details see legend to Fig. 2.

λ_{max} visual pigment and a red R-type oil droplet with a λ_{cut} at 562 nm. Both the principal and accessory members of the double cone pair contained the same 566 nm λ_{max} visual pigment that was also found in the LWS single cones. While the accessory member did not contain an oil droplet, the principal member had a colourless oil droplet with a λ_{cut} at 413 nm.

In the central retina, cone oil droplets appeared either transparent/colourless or pale green (Fig. 1C). The transition from 'normally' pigmented oil droplets located towards the periphery (Fig. 1A) to these less pigmented types in the centre of the visual streak occurred over a short distance

(approximately 50 μm when measured on a flat-mounted retina) on the edges of the visual streak (Figs 1B, 5A). Unlike in the periphery, definitive visual pigment-oil droplet pairings in the central retina/visual streak could not be made because of the smaller size of the cone outer segments (<1 μm diameter where present) and the fact that the retinal tissue was not dispersed in order to preserve orientation. Nevertheless, it is likely that there were several different types of cone in the central retina, each of which contained a different visual pigment, because there were oil droplets of slightly different diameters (Fig. 1C) and with different spectral absorbance characteristics (Fig. 5B). The absorbance spectra of oil droplets measured in the central

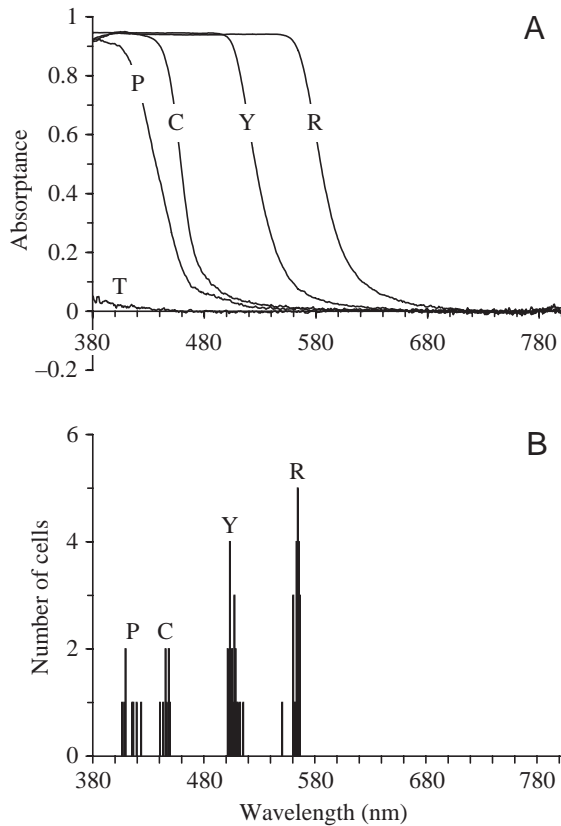


Fig. 4. Mean absorbance spectra of cone photoreceptor oil droplets in the wedge-tailed shearwater *Puffinus pacificus*. (A) Spectra from single and double cones in the peripheral retina, and (B) histogram showing the spectral distribution of the cut-off wavelengths (λ_{cut}) of the oil droplets used to create these mean spectra. T, C, Y, R and P refer to the T-type ('transparent'), C-type ('colourless'), Y-type ('yellow'), R-type ('red') and P-type ('pale/principal') oil droplets found in the VS, SWS, MWS and LWS single cones and the principal member of the LWS double cone pair, respectively.

retina fell into five distinct groups (labeled **t**, **c**, **y**, **r** and **p** in Fig. 5B). The most common droplet type (**p**) had a spectral absorbance (mean λ_{cut} =414 nm, $N=12$) that closely resembled the P-type oil droplets of the principal member of the LWS double cones in the peripheral retina. Transparent oil droplets (**t**) showing no significant absorption across the spectrum were also present, and were identical to the T-type oil droplets associated with the VS visual pigment in the periphery. The remaining three types of oil droplet were classified as **c**, **y** and **r** and were considered to be less pigmented versions of the C-, Y- and R-type oil droplets found in the SWS, MWS and LWS single cones at the periphery. This was deduced by taking the measured absorbance spectra for the central **c**, **y**, and **r** oil droplets (Fig. 5B) and modeling the effect of increasing the density of the carotenoid pigment(s) they contain to levels estimated for the C, Y and R-type oil droplets found in the periphery. The results of this modeling are shown in Fig. 5C. Peak absorbances for the peripheral Y- and R-type oil droplets (16.6 and 2.4, respectively) were estimated from their λ_{cut}

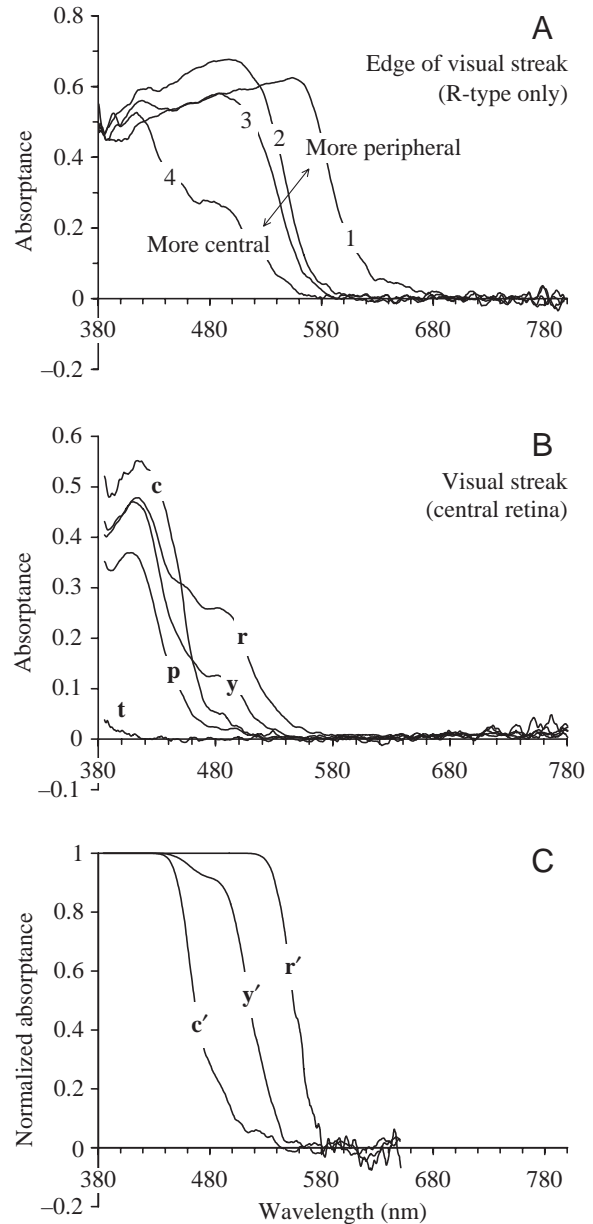


Fig. 5. (A) Absorbance spectra of R-type oil droplets measured on the edge of the visual streak (paired with the LWS visual pigment). 1, more peripheral; 2 and 3, intermediate location; 4, more central. Note that the λ_{cut} of the oil droplets is shifted towards shorter wavelengths the nearer they are to the centre of the visual streak. (B) Absorbance spectra of oil droplets located at the centre of the visual streak. Spectra **t**, **c**, **y** and **r** were used to model quantal sensitivities for VS, SWS, MWS and LWS single cones in the central retina (Fig. 6A). Spectrum **p** corresponds to oil droplets in the principal member of the double cone pair. (C) Modeled absorbance spectra for **c**, **y** and **r** oil droplets in the central retina (Fig. 5B) adjusted for peak absorbances estimated for the C-, Y- and R-type oil droplets in the periphery. See text for more details.

values using the equations given by Lipetz (1984b) for turtle oil droplets. The relationship between C-type oil droplet λ_{cut} and peak absorbance has not been quantified and was taken to be

Table 1. *Microspectrophotometric data for visual pigments and oil droplets measured outside the visual streak*

Visual pigments	Cones				Rods
	VS	SWS	MWS	LWS single/double	
Mean λ_{\max} of pre-bleach absorbance spectra (nm)	406.0±4.2	449.8±3.9	503.1±2.9	566.0±3.3	502.0±1.6
λ_{\max} of mean pre-bleach absorbance spectrum (nm)	405.8	449.9	502.5	567.2	502.3
Mean λ_{\max} of difference spectra (nm)	402.5±1.1	450.9±2.5	505.0±3.1	564.0±5.0	505.1±2.4
λ_{\max} of mean difference spectrum (nm)	403.3	453.2	504.9	566.4	505.6
Absorbance at λ_{\max} of mean difference spectrum	0.015	0.014	0.020	0.022	0.039
Number of cells used in analysis	4	7	7	7	20

Oil droplets (periphery)	T-type	C-type	Y-type	R-type	P-type	
Mean λ_{cut} of absorbance spectra (nm)	<370	445.0±2.8	505.5±3.7	562.4±3.5	412.6±6.1	–
λ_{cut} of mean absorbance spectrum (nm)	<370	445.0	503.6	562.1	411.7	–
Mean λ_{mid} of absorbance spectra (nm)	<370	459.8±2.5	527.7±5.6	586.1±4.5	438.5±5.3	–
λ_{mid} of mean absorbance spectrum (nm)	<370	460.0	527.5	586.3	439.3	–
Mean diameter (μm)	2.8±0.5	3.4±0.4	3.8±0.3	4.2±0.5	3.5±0.4	–
Mean maximum transverse absorbance	<0.05	0.95±0.05	0.95±0.04	0.93±0.05	0.93±0.11	–
Number of oil droplets used in analysis	6	8	20	22	8	–

Values are means \pm 1 s.d.

λ_{\max} , wavelength of maximum absorbance; λ_{cut} , cut-off wavelength; λ_{mid} , wavelength of half maximum measured absorbance.

Avian rods do not contain oil droplets. T-, C-, Y-, R- and P-type oil droplets are located in the VS, SWS, MWS and LWS single cones and the principal member of the LWS double cones, respectively. Spectra of P-type oil droplets did not seem to vary across the retina and the accessory member of the double cones did not contain an oil droplet. Parameters listed are for oil droplets located outside the visual streak.

See list of abbreviations and text for more details.

1.0 for peripheral C-type oil droplets; this value is the lower limit for pigmented droplets in the turtle retina (Lipetz, 1984b). (The peak absorbance of densely pigmented oil droplets cannot be measured accurately with a microspectrophotometer due to the effects of bypassing light (Lipetz, 1984b), which in the current machine limit the upper absorbance values that can be measured to about 0.9 for a 3 μm diameter droplet, as indicated by the flat-topped absorbance spectra for the C-, Y- and R-type oil droplets in Fig. 4A.) Smoothed absorbance spectra for the central **c**, **y**, and **r** oil droplets were converted to absorbance, scaled by a factor equivalent to the ratio of central (measured) oil droplet absorbance to peripheral (estimated) oil droplet absorbance (3.2, 8.5 and 60.3 for the C:c, Y:y and R:r types, respectively) and converted back to absorbance for display. The modeled oil droplets, labeled **c'**, **y'** and **r'** in Fig. 5C, resemble the peripheral C-, Y- and R-type droplets, having λ_{cut} at around 445, 490 and 540 nm, respectively. From Figs 5A,C and 1A–C it seems more than likely that, rather than losing particular cone types, the oil droplets associated with the SWS, MWS and LWS visual pigments gradually reduce their carotenoid pigmentation the nearer they are to the centre of the visual streak.

Spectral transmittance of the ocular media

The method used to measure the spectral transmittance of the ocular media in the anterior segment of the eye was not ideal. More reliable results can be obtained using a spectrophotometer fitted with an integrating sphere (Hart et al., 1998, 1999; Hart, 2002) because light scattered by the tissue

is collected more efficiently. Nevertheless, the method used in this instance was a successful improvisation in the field, the only drawback being that the absolute maximum transmittance of the ocular media could not be determined with sufficient accuracy. For this reason, the averaged transmittance spectrum was normalized to the measured maximum transmittance at long wavelengths. As can be seen from Fig. 6, the ocular media of *P. pacificus* transmits wavelengths down to approximately 300 nm, with a wavelength at 0.5 transmittance ($\lambda_{T0.5}$) of 335 nm.

Cone quantal sensitivities

With the exception of the transparent T-type oil droplet associated with the VS (or UVS) single cones, avian cone oil droplets generally act as long-pass cut-off filters. Consequently, the spectral sensitivity of a given cone is the product of the spectral absorbance of the visual pigment in the outer segment and the spectral transmittance (1-absorbance) of the oil droplet with which it is paired. Relative quantal spectral sensitivities were calculated for single cone photoreceptors in different regions of the wedge-tailed shearwater retina (Fig. 7A,B), as follows. Visual pigment spectral absorbance was modeled using mathematical templates (Govardovskii et al., 2000) of the appropriate λ_{\max} (Table 1). Outer segments were assumed to be 16 μm long (Morris and Shorey, 1967) and contain a visual pigment with a specific (decadic) absorbance of 0.014 μm^{-1} (Bowmaker and Knowles, 1977). Predicted photon catches for each cone type were also adjusted according to the cross-sectional area of

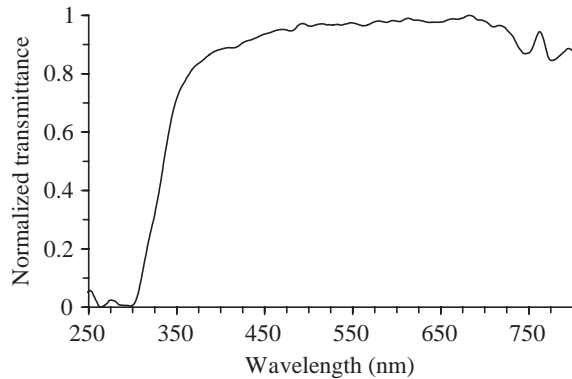


Fig. 6. Spectral transmittance of the ocular media (cornea, aqueous humour and lens) of the eye of the wedge-tailed shearwater *Puffinus pacificus*, measured along the optic axis. The wavelength of 0.5 transmittance ($\lambda_{T0.5}$) was 335 nm.

the relevant oil droplet they contained (Table 1) and the transmittance of the ocular media (Fig. 6). For cones in the peripheral retina (i.e. outside the visual streak; Fig. 1A), the VS, SWS, MWS and LWS cone visual pigments were combined with their corresponding oil droplets, the absorbance spectra of which are labeled T, C, Y and R, respectively, in Fig. 4A. Because the T-type oil droplets do not contain short-wavelength-absorbing carotenoid pigments, the peak sensitivity of the VS cone (407 nm) is very similar to the λ_{\max} of the visual pigment it contains. However, spectral filtering by the C-, Y- and R-type oil droplets shift the peak spectral sensitivities of the SWS, MWS and LWS single cones (472, 538 and 600 nm, respectively; Fig. 7A) to wavelengths longer than the λ_{\max} of their respective visual pigments.

In the central retina, the VS, SWS, MWS and LWS single cones were assumed to contain the t, c, y and r droplets shown in Fig. 5B (see above). Calculated spectral sensitivities are also displayed in Fig. 7A. The spectral location of the peak sensitivity of the VS single cone was the same as in the periphery. However, the reduced pigmentation of the presumptive C-, Y- and R-type oil droplets in the centre of the visual streak results in smaller shifts in the peak sensitivities of the SWS, MWS and LWS single cones towards long wavelengths (466, 512 and 573 nm, respectively). The length of the cone outer segments was assumed to be identical between central and peripheral regions, as appears to be the case for other bird species (e.g. Rojas et al., 1999). Nevertheless, the total photon catch of all single cone types in the centre of the visual streak was less than that at the periphery because of the reduced cross sectional area of the oil droplets (mean diameters 1.4, 2, 2 and 2.1 μm for t, c, y and r oil droplets, respectively), despite the reduction in oil droplet pigmentation (which at the periphery reduces the overall photon catch of the outer segment by 30, 47 and 39%, respectively, for the SWS, MWS and LWS single cones). To further illustrate the transition in cone spectral properties from peripheral to central retina, the spectral sensitivities of LWS

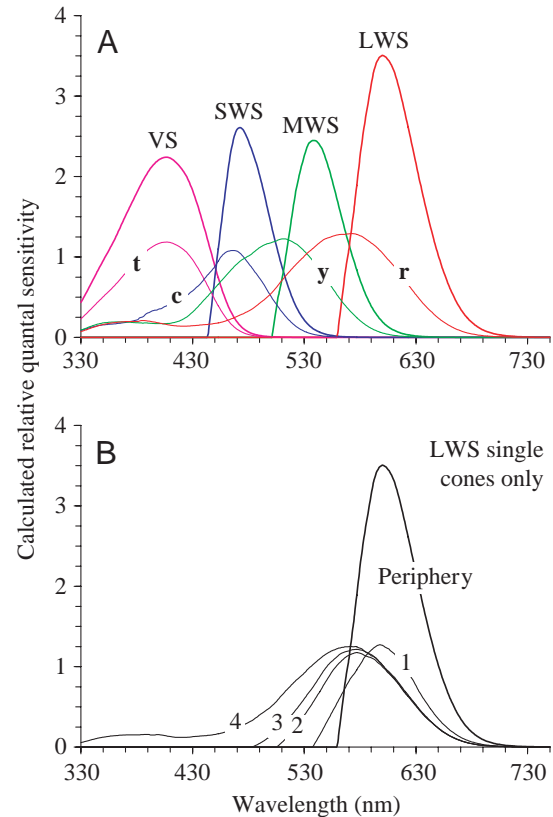


Fig. 7. Calculated relative quantal sensitivities of photoreceptors in different regions of the wedge-tailed shearwater retina. (A) Photoreceptors in the peripheral retina (bold traces) and the centre of the visual streak (thin traces). VS, SWS, MWS and LWS refer to the quantal sensitivities of the four types of single cone in the peripheral retina, calculated using oil droplet spectra T, C, Y and R shown in Fig. 4A, respectively. Labels t, c, y and r refer to quantal sensitivities of the VS, SWS, MWS and LWS single cones in the central retina, calculated using the oil droplet absorbance spectra t, c, y and r shown in Fig. 5B, respectively. (B) LWS single cones at the edge of the visual streak (thin traces) where the 'redness' of the R-type oil droplets fades sharply with decreasing eccentricity. Labels 1–4 refer to calculated quantal sensitivities of LWS visual pigment-containing single cones using oil droplet absorbance spectra 1–4 shown in Fig. 5A. For comparison, the calculated quantal sensitivity of the LWS single cone in the periphery is also shown (bold trace labeled 'Periphery', same as 'LWS' in A). In both A and B, the greater sensitivities of the cones located in the peripheral retina are due to larger oil droplet diameters. See text for more details.

single cones on the edge of the visual streak were also calculated (Fig. 7B, traces 1–4), using the absorbance spectra for oil droplets that changed from red to orange in this retinal area (Fig. 5A, spectra 1–4).

Discussion

Microspectrophotometric data

In general, the retina of the wedge-tailed shearwater is typical of other diurnal birds. It contains rods, double cones

and four types of single cone. Rod, MWS single cone and LWS single/double cone visual pigment λ_{\max} values show relatively little variation between bird species. The biggest interspecific difference is in the λ_{\max} of the visual pigment found in the single cones that contain a T-type oil droplet; values measured microspectrophotometrically range from 359 to 424 nm (for a review, see Hart, 2001b). All of these UVS/VS type visual pigments are thought to belong to the same 'SWS1' opsin class (Yokoyama, 2000) and are conjugated with the same chromophore (11-*cis* retinal). Differences in their λ_{\max} values are, therefore, due only to differences in the amino acid sequence of their opsin protein (Wilkie et al., 1998, 2000; Yokoyama et al., 2000a,b; Hunt et al., 2001). Interestingly, the λ_{\max} of the SWS visual pigment found in the single cones with C-type oil droplets covaries with the λ_{\max} of the SWS1 opsin-based visual pigment found in the UVS/VS single cone, as does the λ_{cut} of the C-type oil droplet and, accordingly, the spectral sensitivity of the SWS single cones (Bowmaker et al., 1997; Hart, 2001b). The strong correlation between UVS/VS single cone and SWS single cone spectral sensitivities suggests that avian photoreceptors are tuned to optimize the extraction of chromatic information over a given spectral range, the short wavelength limit of which varies between species.

With a λ_{\max} at 406 nm, the VS visual pigment of the wedge-tailed shearwater is similar to the only other marine birds for which data are available, the Manx shearwater *Puffinus puffinus* (402 nm λ_{\max} ; Bowmaker et al., 1997) and the Humboldt penguin *Spheniscus humboldti* (403 nm λ_{\max} ; Bowmaker and Martin, 1985). This type of VS visual pigment, which differs subtly from those found in anseriform and galliform species (λ_{\max} 415–426 nm), is also found in the ostrich *Struthio camelus* (405 nm λ_{\max} ; Wright and Bowmaker, 2001) and the feral pigeon *Columba livia* (409 nm λ_{\max} ; Bowmaker et al., 1997) and so is not exclusive to marine bird species. On the basis of SWS1 opsin DNA sequences, Ödeen and Håstad (2003) have suggested that the distribution of UVS/VS visual pigment λ_{\max} values among bird species is complex and probably reflects ecological adaptations rather than phylogenetic relatedness, as seems to be the case for cone photoreceptor abundance (Goldsmith et al., 1984; Partridge, 1989; Hart, 2001a). There are likely to be many different adaptive reasons for a particular complement of photoreceptor spectral sensitivities, depending, for example, on the physical habitat and foraging or predator avoidance behaviours of a given species.

As an oceanic marine bird, the visual system of the wedge-tailed shearwater appears to be well adapted to its photic environment. Shearwaters use a variety of strategies to capture their prey, which consists largely of fish, squid and crustaceans (Nelson, 1980), but feed mainly while floating on the water or during shallow dives made either from the surface or a short distance above it (Warham, 1990). They must, therefore, be able to detect their prey through the air–water interface, although this is a complex visual task: plunge-diving birds most cope not only with the effects of refraction on the apparent position of the prey item underwater (Katzir, 1993),

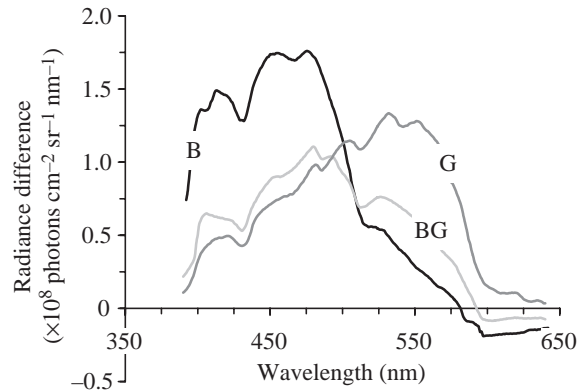


Fig. 8. Optimal wavelength ranges for through-surface vision for three different water types: blue (B), blue-green (BG) and green (G). Each line was generated by subtracting the surface-reflected radiance spectrum from the spectral radiance of the upwelling light, using data from Austin (1974). A visual system most sensitive to wavelengths in which the upwelling light is relatively rich compared to the surface reflectance would be better suited for through-surface vision (Lythgoe, 1979). The wedge-tailed shearwater inhabits predominantly blue oceanic water; the optimal wavelengths for through surface vision in this photic environment are approximately 400–500 nm.

but also with specular reflection of skylight from the surface that interposes a contrast-reducing glare (Lythgoe, 1979). Reflections from the surface of the water have the same spectral distribution as skylight, but the spectral radiance of the upwelling light from the ocean – against which prey must be detected – is dominated by the absorption and scatter of the water (Austin, 1974). Considering this phenomenon, Lythgoe (1979) proposed that a visual system most sensitive to wavelengths in which the upwelling light is rich, and the surface reflectance relatively poor, would be adaptive for through-surface vision.

The spectral distribution of upwelling light from a body of water depends on the amount of particulate matter, dissolved organic compounds and chlorophyll it contains. Different types of water have different levels of these substances and, accordingly, different upwelling spectral radiances or 'colours' (Austin, 1974; Jerlov, 1976). Fig. 8 shows the calculated difference between upwelling and surface-reflected radiances for three different water types: 'blue', 'blue-green' and 'green', calculated from data in Austin (1974). The geographical range of the wedge-tailed shearwater extends throughout the tropical and subtropical Indian and Pacific Oceans (del Hoyo et al., 1992). Consequently, they forage mainly over oceanic 'blue' water types (Jerlov types I, IA and IB; Jerlov, 1976) whose upwelling spectral radiance is relatively richer in short wavelengths between about 400 and 500 nm (Fig. 8). Below 400 nm, submerged objects would become increasingly difficult to distinguish against the surface glare and the 406 nm λ_{\max} VS visual pigment of the wedge-tailed shearwater would, therefore, be more useful than a UVS-type visual pigment ($\lambda_{\max} < 400$ nm) for through surface vision. It is also interesting

to note that the proportion of VS cones in the wedge-tailed shearwater retina (approximately 16% of all cone types) is at least twice as high as in many terrestrial bird species (e.g. Goldsmith et al., 1984; Hart et al., 1998, 2000b; Wright and Bowmaker, 2001) and marine species (e.g. silver gull *Larus novaehollandiae*, noddy tern *Anous minutus*) that surface seize but do not plunge dive (Hart, 2001a). Moreover, despite their suggested role in movement detection (Campenhausen and Kirschfeld, 1998), the retinæ of blue-water marine birds generally contain a lower proportion of double cones (wedge-tailed shearwater 34%, silver gull 30%, noddy tern 29%) compared to terrestrial species (range 35–56%; Hart, 2001a), possibly because their long-wavelength sensitivity is less useful for through-water vision.

The LWS visual pigment of the wedge-tailed shearwater has a similar λ_{\max} (566 nm) to other terrestrial bird species (see Hart, 2001b) and is not shifted towards shorter wavelengths as in the Humboldt penguin *Spheniscus humboldti* (Bowmaker and Martin, 1985). The 543 nm λ_{\max} LWS visual pigment of the penguin is presumably an adaptation to the restricted spectral bandwidth it encounters when foraging in the ocean at depths of 30 m or more (Williams, 1995), where longer wavelengths are attenuated more rapidly than shorter wavelengths with increasing depth (Jerlov, 1976). Plunge-diving shearwaters, on the other hand, take most of their prey within 2 m of the surface (Warham, 1990) where the spectral distribution of light available for vision is less restricted.

The wedge-tailed shearwater retina has a distinct *area centralis horizontalis* or visual streak running horizontally across the retina. A similar band of increased cell density – with or without a central fovea – has been shown, either anatomically or ophthalmoscopically, in several other procellariiform species: the sooty albatross *Phoebastria fusca*, shy albatross *Diomedea cauta*, Manx shearwater *Puffinus puffinus*, sooty shearwater *Puffinus griseus*, soft-plumaged petrel *Pterodroma mollis*, Fulmar petrel *Fulmaris glacialis* and giant petrel *Macronectes giganteus* (Wood, 1917; O'Day, 1940; Lockie, 1952; Hayes and Brooke, 1990). Some shearwaters, for example the little shearwater *Puffinus assimilis*, lack a visual streak and instead have a simple *area centralis*; differences in the retinal topography of petrel species are undoubtedly related to visual ecology, most likely feeding behaviour (Hayes and Brooke, 1990).

Several specialized functions have been attributed to linear areas in birds and other animals, including movement detection, spatial orientation and fixation of the horizon (reviewed in Meyer, 1977). Measurements of the visual fields of the Manx shearwater eye reveal that the long axis of the visual streak is aligned parallel to the physical horizon (Martin and Brooke, 1991), as is the case for other animals that inhabit open, relatively featureless environments (Hughes, 1977; Meyer, 1977). The region of visual space from just above the horizon to just below it will be of great significance to birds such as shearwaters in finding food. Shearwaters usually forage within 10 m of the water's surface (Haney et al., 1992) and search for prey solitarily, only converging to form flocks when

a source of food is located and an individual is observed dropping to the surface to feed (Warham, 1990). Haney et al. (1992) calculated that the mean horizontal distance over which procellariiform seabirds were recruited visually to a feeding flock was around 4.5 km and even proposed a theoretical limit of 20–30 km. It is evident, therefore, that a visual streak sampling the physical horizon with a high spatial resolving power would be adaptive for the detection of potential food sources on the open ocean.

The most intriguing feature of the wedge-tailed shearwater retina is that the pigmented cone oil droplets lose their coloration in the central area of the visual streak. These pale-coloured oil droplets in the visual streak are of marginally different sizes (Fig. 1C) and have slightly different absorbance spectra (Fig. 5B). Moreover, the transition from brightly coloured to almost colourless droplets can be seen at the edge of the visual streak (Figs 1B, 5A). It seems likely, therefore, that rather than only one cone type being present at the centre of the visual streak, all different types of cone are present, but contain oil droplets with absorbance spectra that are different from those in the peripheral retina. This has also been observed in other species that have very small, densely packed photoreceptors in their central retina, e.g. sacred kingfisher *Todiramphus sanctus* (Hart, 2001a) and laughing kookaburra *Dacelo novaeguineae* (N. S. Hart, unpublished). Pigmented oil droplets act as long-pass cut-off filters, blocking almost all light below a critical wavelength (λ_{cut}). Consequently, the effect of a coloured oil droplet on a given cone type is to narrow its spectral sensitivity function, shift the peak sensitivity to a wavelength longer than the λ_{\max} of the visual pigment it contains and reduce the overall photon catch (Bowmaker, 1977). From the predicted spectral sensitivities of the cone photoreceptors in the wedge-tailed shearwater retina (Fig. 7A), it is evident that the reduction of spectral filtering by oil droplets in the central retina results in greater overlap between adjacent spectral classes and a shift in the peak sensitivity of the SWS, MWS and LWS single cone types towards shorter wavelengths compared to those at the periphery. Reduced overlap of adjacent cone spectral sensitivities is thought to improve the discrimination of broadband ('natural') reflectance spectra and enhance colour constancy (Govardovskii, 1983; Vorobyev, 1997, 2003; Vorobyev et al., 1998). However, the benefits of spectral filtering by oil droplets are strongly dependent on light intensity because they reduce the overall quantum catch of the cone and, accordingly, increase photoreceptor signal noise. In the wedge-tailed shearwater retina, the cones become narrower and more densely packed with decreasing eccentricity (Fig. 1), presumably to enhance spatial acuity in the visual streak. The associated decrease in photon capture area results in a lower quantal sensitivity compared to peripheral cones (Fig. 7A), despite the reduction in oil droplet pigmentation. Moreover, ganglion cells in retinal regions of high spatial acuity, such as the visual streak, tend to have smaller receptive fields (Rodieck, 1973), receive inputs from fewer cones (e.g. Manx shearwater; Lockie, 1952) and, consequently, have a lower

signal-to-noise ratio than ganglion cells in the periphery. Theoretical models suggest that the benefit of coloured oil droplets for colour discrimination is marginal at lower light intensities (Vorobyev, 2003). This trade-off between spatial acuity (small cones, low summation) and contrast sensitivity (big cones, high summation) may preclude the presence of highly pigmented oil droplets in centrally located cones because they would further reduce quantum catch below a particular noise threshold. This is probably also the reason why nocturnal and crepuscular species of bird do not have highly pigmented droplets (Muntz, 1972; Bowmaker and Martin, 1978).

If, as in chickens *Gallus gallus* (Osorio et al., 1999), outputs from the four single cone types in the wedge-tailed shearwater retina are compared using opponent mechanisms in a tetrachromatic colour vision system, a coloured object whose image falls on the photoreceptors in the visual streak will produce different cone opponent signals than if it fell on the peripheral retina, especially if its reflectance is rich in short wavelengths of light. Whether or not the neural circuitry of the opponent mechanisms compensates for this topographic variation in colour perception is unknown and this is clearly an area for future study.

List of abbreviations

CCD	charge-coupled device
f	focal length
IR	infrared
LED	light emitting diode
LWS	long-wavelength sensitive
MSP	microspectrophotometer
MWS	medium-wavelength sensitive
NA	numerical aperture
PBS	phosphate-buffered saline
PMT	photomultiplier
SMA	sub-miniature type A connector
SWS	short-wavelength sensitive
UVS	ultraviolet-sensitive
VS	violet sensitive
λ_{cut}	cut-off wavelength (oil droplet)
λ_{max}	wavelength of maximum absorbance (visual pigment)
λ_{mid}	wavelength of half maximum-measured absorbance (oil droplet)
$\lambda_{T0.5}$	wavelength of 0.5 transmittance (ocular media)

The author thanks Prof. David Vaney, Prof. Justin Marshall and Dr Julia Shand (who all donated equipment used in the construction of the microspectrophotometer), Dr Misha Vorobyev, the staff of Heron Island Research Station and the Queensland Parks and Wildlife Service. The author was funded by a University of Queensland (UQ) Postdoctoral Research Fellowship and a UQ New Staff Start-up Grant. All experiments complied with the 'Principals of Animal Care', publication No. 86-23, revised 1985, of the National Institute of Health.

References

- Austin, R. W. (1974). The remote sensing of spectral radiance from below the ocean surface. In *Optical Aspects of Oceanography* (ed. N. G. Jerlov and E. Steemann Nielsen), pp. 317-344. London: Academic Press.
- Bowmaker, J. K. (1977). The visual pigments, oil droplets and spectral sensitivity of the pigeon. *Vision Res.* **17**, 1129-1138.
- Bowmaker, J. K., Heath, L. A., Wilkie, S. E. and Hunt, D. M. (1997). Visual pigments and oil droplets from six classes of photoreceptor in the retinas of birds. *Vision Res.* **37**, 2183-2194.
- Bowmaker, J. K. and Knowles, A. (1977). The visual pigments and oil droplets of the chicken retina. *Vision Res.* **17**, 755-764.
- Bowmaker, J. K. and Martin, G. R. (1978). Visual pigments and colour vision in a nocturnal bird, *Strix aluco* (tawny owl). *Vision Res.* **18**, 1125-1130.
- Bowmaker, J. K. and Martin, G. R. (1985). Visual pigments and oil droplets in the penguin, *Spheniscus humboldti*. *J. Comp. Physiol. A* **156**, 71-77.
- Campenhausen, M. v. and Kirschfeld, K. (1998). Spectral sensitivity of the accessory optic system of the pigeon. *J. Comp. Physiol. A* **183**, 1-6.
- del Hoyo, J., Elliot, A. and Sargatal, J. (1992). *Handbook of the Birds of the World*. Vol. 1. *Ostrich to Ducks*. Barcelona: Lynx Edicions.
- Goldsmith, T. H., Collins, J. S. and Licht, S. (1984). The cone oil droplets of avian retinas. *Vision Res.* **24**, 1661-1671.
- Govardovskii, V. I. (1983). On the role of oil drops in colour vision. *Vision Res.* **23**, 1739-1740.
- Govardovskii, V. I., Fyhrquist, N., Reuter, T., Kuzmin, D. G. and Donner, K. (2000). In search of the visual pigment template. *Vis. Neurosci.* **17**, 509-528.
- Haney, J. C., Fristrup, K. M. and Lee, D. S. (1992). Geometry of visual recruitment by seabirds to ephemeral foraging flocks. *Ornis Scand.* **23**, 49-62.
- Hart, N. S. (1998). *Avian Photoreceptors*. Bristol, UK: University of Bristol, UK.
- Hart, N. S. (2001a). Variations in cone photoreceptor abundance and the visual ecology of birds. *J. Comp. Physiol. A* **187**, 685-697.
- Hart, N. S. (2001b). The visual ecology of avian photoreceptors. *Prog. Ret. Eye Res.* **20**, 675-703.
- Hart, N. S. (2002). Vision in the peafowl (Aves: *Pavo cristatus*). *J. Exp. Biol.* **205**, 3925-3935.
- Hart, N. S., Partridge, J. C., Bennett, A. T. D. and Cuthill, I. C. (2000a). Visual pigments, cone oil droplets and ocular media in four species of estrildid finch. *J. Comp. Physiol. A* **186**, 681-694.
- Hart, N. S., Partridge, J. C. and Cuthill, I. C. (1998). Visual pigments, oil droplets and cone photoreceptor distribution in the European starling (*Sturnus vulgaris*). *J. Exp. Biol.* **201**, 1433-1446.
- Hart, N. S., Partridge, J. C. and Cuthill, I. C. (1999). Visual pigments, cone oil droplets, ocular media and predicted spectral sensitivity in the domestic turkey (*Meleagris gallopavo*). *Vision Res.* **39**, 3321-3328.
- Hart, N. S., Partridge, J. C., Cuthill, I. C. and Bennett, A. T. (2000b). Visual pigments, oil droplets, ocular media and cone photoreceptor distribution in two species of passerine bird: the blue tit (*Parus caeruleus* L.) and the blackbird (*Turdus merula* L.). *J. Comp. Physiol. A* **186**, 375-387.
- Hayes, B. P. and Brooke, M. d. L. (1990). Retinal ganglion cell distribution and behaviour in procellariiform seabirds. *Vision Res.* **30**, 1277-1289.
- Hughes, A. (1977). The topography of vision in mammals of contrasting life styles: comparative optics and retinal organisation. In *The Visual System in Vertebrates*, vol. VII / 5 (ed. F. Crescitelli), pp. 613-756. Berlin: Springer-Verlag.
- Hunt, D. M., Wilkie, S. E., Bowmaker, J. K. and Poopalasundaram, S. (2001). Vision in the ultraviolet. *Cell. Mol. Life Sci.* **58**, 1583-1598.
- Jerlov, N. G. (1976). *Marine Optics*. Amsterdam: Elsevier Scientific Publishing Company.
- Katzir, G. (1993). Visual mechanisms of prey capture in water birds. In *Vision, Brain and Behavior in Birds* (ed. H. P. Zeigler and H.-J. Bischof), pp. 301-315. Cambridge, Massachusetts: MIT Press.
- Levine, J. S. and MacNichol, E. F., Jr (1985). Microspectrophotometry of primate photoreceptors: art, artefact and analysis. In *The Visual System* (ed. A. Fein and J. S. Levine), pp. 73-87. New York: Liss.
- Liebman, P. A. (1972). Microspectrophotometry of photoreceptors. In *Photochemistry of Vision*, vol. VII / 1 (ed. H. J. A. Dartnall), pp. 481-528. Berlin: Springer-Verlag.
- Lipetz, L. E. (1984a). A new method for determining peak absorbance of dense pigment samples and its application to the cone oil droplets of *Emydoidea blandingii*. *Vision Res.* **24**, 567-604.

- Lipetz, L. E.** (1984b). Pigment types, densities and concentrations in cone oil droplets of *Emydoidea blandingii*. *Vision Res.* **24**, 605-612.
- Lockie, J. D.** (1952). A comparison of some aspects of the retinae of the Manx shearwater, fulmar petrel and house sparrow. *Quart. J. Microsc. Sci.* **93**, 347-356.
- Lythgoe, J. N.** (1979). *The Ecology of Vision*. Oxford: Oxford University Press.
- MacNichol, E. F., Jr.** (1986). A unifying presentation of photopigment spectra. *Vision Res.* **26**, 1543-1556.
- Martin, G. R.** (1985). Eye. In *Form and Function in Birds*, vol. 3 (ed. A. S. King and J. McLelland), pp. 311-373. London: Academic Press.
- Martin, G. R.** (1998). Eye structure and amphibious foraging in albatrosses. *Proc. R. Soc. Lond. B* **265**, 665-671.
- Martin, G. R.** (1999). Eye structure and foraging in King Penguins *Aptenodytes patagonicus*. *Ibis* **141**, 444-450.
- Martin, G. R. and Brooke, M. d. L.** (1991). The eye of a procellariiform seabird, the Manx shearwater, *Puffinus puffinus*: visual fields and optical structure. *Brain Behav. Evol.* **37**, 65-78.
- Martin, G. R. and Prince, P. A.** (2001). Visual fields and foraging in procellariiform seabirds: sensory aspects of dietary segregation. *Brain Behav. Evol.* **57**, 33-38.
- Meyer, D. B.** (1977). The avian eye and its adaptations. In *The Visual System in Vertebrates*, vol. VII / 5 (ed. F. Crescitelli), pp. 549-611. Berlin: Springer-Verlag.
- Morris, V. B. and Shorey, C. D.** (1967). An electron microscope study of types of receptor in the chick retina. *J. Comp. Neurol.* **129**, 313-340.
- Muntz, W. R. A.** (1972). Inert absorbing and reflecting pigments. In *Photochemistry of Vision*, vol. VII / 1 (ed. H. J. A. Dartnall), pp. 529-565. Berlin: Springer-Verlag.
- Nelson, B.** (1980). *Seabirds: Their Biology and Ecology*. London: Hamlyn.
- O'Day, K.** (1940). The fundus and fovea centralis of the albatross (*Diomedea cauta cauta* - Gould). *Br. J. Ophthalmol.* **24**, 201-207.
- Ödeen, A. and Håstad, O.** (2003). Complex distribution of avian color vision systems revealed by sequencing the SWS1 opsin from total DNA. *Mol. Biol. Evol.* **20**, 855-861.
- Osorio, D., Vorobyev, M. and Jones, C. D.** (1999). Colour vision of domestic chicks. *J. Exp. Biol.* **202**, 2951-9.
- Partridge, J. C.** (1989). The visual ecology of avian cone oil droplets. *J. Comp. Physiol. A* **165**, 415-426.
- Rochon-Duvigneaud, A.** (1943). *Les Yeux et la Vision des Vertébrés*. Paris: Masson.
- Rodieck, R. W.** (1973). *The Vertebrate Retina*. San Francisco: W. H. Freeman and Company.
- Rojas, L. M., McNeil, R., Cabana, T. and Lachapelle, P.** (1999). Behavioral, morphological and physiological correlates of diurnal and nocturnal vision in selected wading bird species. *Brain, Behav. Evol.* **53**, 227-242.
- Schodde, R. and Tidemann, S. C.** (1997). *Reader's Digest Complete Book of Australian Birds*. Sydney: Reader's Digest (Australia) Pty Ltd.
- Sivak, J. G.** (1976). The role of the flat cornea in the amphibious behaviour of the black-footed penguin, *Spheniscus demersus*. *Can. J. Zool.* **54**, 1341-1345.
- Sivak, J. G., Howland, H. C. and McGill-Harelstad, P.** (1987). Vision of the Humboldt penguin (*Spheniscus humboldti*) in air and water. *Proc. R. Soc. Lond. B* **229**, 467-472.
- Sivak, J. G., Lincer, J. L. and Bobier, W.** (1977). Amphibious visual optics of the eyes of the double-crested cormorant (*Phalacrocorax auritus*) and the brown pelican (*Pelecanus occidentalis*). *Can. J. Zool.* **55**, 782-788.
- Slonaker, J. R.** (1897). A comparative study of the area of acute vision in vertebrates. *J. Morphol.* **13**, 445-493.
- Vorobyev, M.** (1997). Costs and benefits of increasing the dimensionality of colour vision system. In *Biophysics of Photoreception: Molecular and Phototransductive Events* (ed. C. Taddei-Ferretti), pp. 280-289. Singapore: World Scientific.
- Vorobyev, M.** (2003). Coloured oil droplets enhance colour discrimination. *Proc. R. Soc. Lond. B* **270**, 1255-1261.
- Vorobyev, M., Osorio, D., Bennett, A. T., Marshall, N. J. and Cuthill, I. C.** (1998). Tetrachromacy, oil droplets and bird plumage colours. *J. Comp. Physiol. A* **183**, 621-633.
- Walls, G. L.** (1942). *The Vertebrate Eye and its Adaptive Radiation*. New York: Hafner.
- Warham, J.** (1990). *The Petrels: Their Ecology and Breeding Systems*. London: Academic Press.
- Wilkie, S. E., Robinson, P. R., Cronin, T. W., Poopalasundaram, S., Bowmaker, J. K. and Hunt, D. M.** (2000). Spectral tuning of avian violet- and ultraviolet-sensitive visual pigments. *Biochemistry* **39**, 7895-7901.
- Wilkie, S. E., Vissers, P. M., Das, D., Degrip, W. J., Bowmaker, J. K. and Hunt, D. M.** (1998). The molecular basis for UV vision in birds: spectral characteristics, cDNA sequence and retinal localization of the UV-sensitive visual pigment of the budgerigar (*Melopsittacus undulatus*). *Biochem. J.* **330**, 541-547.
- Williams, T. D.** (1995). *The Penguins: Spheniscidae*. Oxford: Oxford University Press.
- Wood, C. A.** (1917). *The Fundus Oculi of Birds Especially as Viewed by the Ophthalmoscope*. Chicago: Lakeside Press.
- Wright, M. W. and Bowmaker, J. K.** (2001). Retinal photoreceptors of paleognathous birds: the ostrich (*Struthio camelus*) and rhea (*Rhea americana*). *Vision Res.* **41**, 1-12.
- Yokoyama, S.** (2000). Molecular evolution of vertebrate visual pigments. *Progr. Ret. Eye Res.* **19**, 385-419.
- Yokoyama, S., Blow, N. S. and Radlwimmer, F. B.** (2000a). Molecular evolution of color vision of zebra finch. *Gene* **259**, 17-24.
- Yokoyama, S., Radlwimmer, F. B. and Blow, N. S.** (2000b). Ultraviolet pigments in birds evolved from violet pigments by a single amino acid change. *Proc. Natl. Acad. Sci. USA* **97**, 7366-7371.